

## Understanding Central Spin Decoherence Due to Interacting Dissipative Spin Baths

Mykyta Onizhuk<sup>1</sup>, Yu-Xin Wang (王语馨)<sup>1,2</sup>, Jonah Nagura<sup>1</sup>, Aashish A. Clerk<sup>1</sup>, and Giulia Galli<sup>1,3,4,\*</sup>

<sup>1</sup>*Pritzker School of Molecular Engineering, University of Chicago, Chicago, Illinois 60637, USA*

<sup>2</sup>*Joint Center for Quantum Information and Computer Science, University of Maryland, College Park, Maryland 20742, USA*

<sup>3</sup>*Department of Chemistry, University of Chicago, Chicago, Illinois 60637, USA*

<sup>4</sup>*Materials Science Division and Center for Molecular Engineering, Argonne National Laboratory, Lemont, Illinois 60439, USA*

 (Received 8 December 2023; revised 30 April 2024; accepted 20 May 2024; published 18 June 2024)

We propose a new approach to simulate the decoherence of a central spin coupled to an interacting dissipative spin bath with cluster-correlation expansion techniques. We benchmark the approach on generic 1D and 2D spin baths and find excellent agreement with numerically exact simulations. Our calculations show a complex interplay between dissipation and coherent spin exchange, leading to increased central spin coherence in the presence of fast dissipation. Finally, we model near-surface nitrogen-vacancy centers in diamond and show that accounting for bath dissipation is crucial to understanding their decoherence. Our method can be applied to a variety of systems and provides a powerful tool to investigate spin dynamics in dissipative environments.

DOI: [10.1103/PhysRevLett.132.250401](https://doi.org/10.1103/PhysRevLett.132.250401)

Understanding the dynamical properties of open many-body quantum systems is a problem of fundamental importance in modern physics [1–6]. The interaction of a quantum system with an environment may radically change its behavior; for example, dissipation may drive novel phase transitions [7,8], stabilize exotic states or subspaces [9–11], and lead to rich spectral statistics [12]. Recent experimental advances have enabled the ability to engineer dissipative environments [13], as well as probe environmental effects via a single two-level system [6,14,15]. Specifically, sensing using single electron spins in solids has emerged as a hallmark near-term quantum technology, with applications in physics, chemistry, and biology [16,17].

Generic quantum sensing protocols seek to recover the dynamics of a many-body system from the dephasing of a two-level probe [18,19]. To shed light on the main mechanisms determining the sensing signal, one requires accurate computational methods to simulate the full dephasing dynamics generated by an interacting, many-body open quantum system. One may then use such computational techniques to solve a broad range of problems in materials science and quantum many-body physics.

In the case of closed quantum systems, the dynamical evolution of a two-level system (a central spin) coupled to a spin bath can be studied with the cluster-correlation expansion (CCE) technique [20], which produces accurate results for many physical systems [21–24]. While alternate cluster techniques for translationally invariant systems have been used to study dissipative steady states [25], a more general method to investigate the dynamics of open quantum systems is not yet available.

In this Letter, we propose a novel approach for simulating dissipative, interacting spin baths and their impact on

the central spin coherence evolution by solving many-body Lindblad master equations (ME) using CCE techniques. We benchmark the method against exact numerical simulations of baths formed by 1D and 2D spin lattices with variable dissipation rates and also present results for realistic, experimentally motivated dissipative spin systems.

*Theoretical framework.*—We study the dynamics of a central spin coupled to an interacting spin bath with Markovian dissipation, as described by the Gorini-Kossakowski-Sudarshan-Lindblad (Lindblad) ME [26,27] (in units  $\hbar = 1$ ),

$$\frac{d}{dt}\hat{\rho}(t) = -i[\hat{H}, \hat{\rho}(t)] + \sum_i \gamma_i \mathcal{D}[\hat{L}_i](\hat{\rho}), \quad (1)$$

where  $\hat{H} = (\hat{\sigma}_z/2) \otimes \hat{B} + \hat{H}_{\text{bath}}$  is a pure dephasing interaction between the central spin and the bath operator  $\hat{B}$ ,  $\hat{H}_{\text{bath}}$  describes intrabath interactions,  $\mathcal{D}[\hat{L}_i](\hat{\rho}) \equiv \hat{L}_i \hat{\rho} \hat{L}_i^\dagger - \frac{1}{2} \{ \hat{L}_i^\dagger \hat{L}_i, \hat{\rho} \}$  are superoperators accounting for incoherent processes between the bath and the external Markovian environment, and  $\hat{L}_i$  are bath jump operators. Note that we do not assume the spin bath is translationally invariant or has a permutation symmetry. We omit any direct dephasing of the central spin (due to coupling to its own Markovian environment), as such dynamics can always be trivially factored out from the coherence.

The coherence function  $\mathcal{L}(t)$  is defined as the normalized off-diagonal spin density matrix element  $\mathcal{L}(t) = \text{Tr}[\hat{\rho}_{01}(t)] / \text{Tr}[\hat{\rho}_{01}(0)]$ , where  $\hat{\rho}_{01}(t) = \langle 0 | \hat{\rho}(t) | 1 \rangle$  is a partial inner product of the total density matrix, and  $|0\rangle, |1\rangle$  are  $\hat{\sigma}_z$  eigenstates of the central spin.

Starting from Eq. (1), the evolution of the  $\hat{\rho}_{01}(t)$  is computed by solving [28]

$$\frac{d\hat{\rho}_{01}}{dt} = -i\hat{H}^{(0)}\hat{\rho}_{01} + i\hat{\rho}_{01}\hat{H}^{(1)} + \sum_i \gamma_i \mathcal{D}[\hat{L}_i](\hat{\rho}_{01}), \quad (2)$$

where  $\hat{H}^{(a)} = \langle \alpha | \hat{H} | \alpha \rangle$  are effective Hamiltonians projected on the central spin states  $|\alpha\rangle$ .

Using the CCE method, one approximates the coherence function of the central spin interacting with the spin bath  $\mathcal{L}(t)$  as a product of irreducible cluster contributions  $\mathcal{L}_C(t)$  [20,33],

$$\mathcal{L}(t) = \prod_C \tilde{\mathcal{L}}_C(t) = \prod_i \tilde{\mathcal{L}}_{\{i\}}(t) \prod_{i,j} \tilde{\mathcal{L}}_{\{ij\}}(t) \dots, \quad (3)$$

where the product goes over single bath spins  $i$ , pairs  $i, j$ , and larger cluster sizes up to a given cutoff. Largest size of the cluster defines the order of the approximation used. Each of the contributions is defined recursively from the coherence of the central spin, interacting with a single cluster  $C$ ,

$$\tilde{\mathcal{L}}_C(t) = \frac{\mathcal{L}_C(t)}{\prod_{C'} \tilde{\mathcal{L}}_{C'C}(t)}, \quad (4)$$

where  $C'$  indicates all subclusters of the cluster  $C$ . Conventionally, one computes the cluster coherence functions  $\mathcal{L}_C(t)$  by solving the Schrodinger equation of the central spin coupled to a cluster [20]. Here, instead, we use Eq. (2) to compute the cluster contributions in Eq. (4) to account for the impact of both dissipative and coherent intrabath dynamics on the central spin coherence. We thus reduce the solution of a single intractable Lindbladian to a number of master equations of finite size equal to the order of the cluster expansion. We refer to such an approach as ME-CCE.

It is worth contrasting our method with a broad class of approximations based on truncating equations of motions for multiparticle correlators at some finite order  $n$ . This includes truncated cumulant expansions for spin systems [34], the Bogoliubov backreaction method for interacting bosons [35,36], and other approaches based on truncating the infinite Bogoliubov-Born-Green-Kirkwood-Yvon hierarchy. These methods involve solving a large system of coupled nonlinear differential equations, which becomes unwieldy for large systems and at higher order. In contrast, our method targets a specific observable of interest and only involves solving a number of *independent* linear ordinary differential equations (corresponding to dynamics of independent fixed-sized clusters). The ME-CCE approach is thus significantly easier to implement at higher orders and provides a versatile framework for studying open many-body quantum dynamics relevant to near-term quantum technologies.

*Results.*—We start by benchmarking our method and first consider its general convergence properties. At short evolution times  $t$  satisfying  $\max_\alpha (\|\hat{H}^{(\alpha)}\|)t \ll 1$  and  $\max_i (\gamma_i \|\hat{L}_i^\dagger \hat{L}_i\|)t \ll 1$ , with  $\|\cdot\|$  denoting the Frobenius operator norm, the ME-CCE method rapidly converges and the CCE may be truncated at a relatively low order, similar to conventional CCE calculations [28]. However, at longer times the order of truncation adopted in numerical simulations needs to be carefully checked in each specific case and depends on the parameter regime of interest.

We investigate the validity of our approach for the paradigmatic example of a central spin- $\frac{1}{2}$  coupled to a low-dimensional spin bath with local thermal baths and dipolar interactions. We write the resulting XXZ-Hamiltonian under the secular approximation as

$$\hat{H}^{(0/1)} = \sum_{i=1}^n \pm \frac{a_i}{2} \hat{\Gamma}_z^i + \sum_{i,j} \frac{J_{ij}}{2} (\hat{\Gamma}_+^i \hat{\Gamma}_-^j + \hat{\Gamma}_-^i \hat{\Gamma}_+^j - 4\hat{\Gamma}_z^i \hat{\Gamma}_z^j), \quad (5)$$

where  $\hat{\Gamma}^i$  are spin- $\frac{1}{2}$  operators of the  $i$ th bath spin,  $a_i$  are coupling of the  $i$ -bath spin to the central spin,  $J_{ij}$  are dipolar couplings between nearest neighbors on the lattice. The evolution of each cluster is computed with Eq. (2), with  $\hat{L}_{i,\pm} = \hat{\Gamma}_{\pm}^i$  as the bath spin jump operators. While our approach is fully general, for illustrative purposes, we consider the experimentally motivated regime where the bath is in the large-temperature limit. In this case, all bath spins thermalize into a maximally mixed state, and the raising and lowering spin jump operators have the same rate  $\gamma_+ = \gamma_- = \gamma$  (for examples outside of this regime see [28]).

Consider first a one-dimensional spin chain as the bath (Fig. 1) in a parameter regime where the conventional CCE is expected to converge efficiently, i.e., the couplings  $a_i$  are significantly larger than the intrabath interactions  $J_{ij}$  [20]. The  $a_i$  and  $J_{ij}$  are chosen randomly, and the bath is initially quenched into a Néel state. We compare our results with the exact numerical simulation of the time evolution of a 12-spin chain. If the spin bath is not dissipative, the CCE approach reproduces the exact dynamics at short timescales but shows deviation from the exact results at longer times, as expected. Increasing the order of the CCE approach reliably yields increasingly accurate results [Fig. 1(b)].

We observe a similar behavior in the system with dissipative spins. The decay rate  $\gamma$  is chosen to obtain sizeable contributions to the decoherence from both coherent and incoherent interactions in the bath [see Fig. 1(c)]. The ME-CCE coherence curve agrees well with the predictions of the direct numerical simulations at higher orders of the approximation.

We further test the predictions of our approach by simulating various pulse sequences applied to the central spin. Figure 2(a) shows the comparison between the ME-CCE and the full numerical predictions for the dynamical-decoupling sequences with one ( $p = 1$ , Hahn echo), and

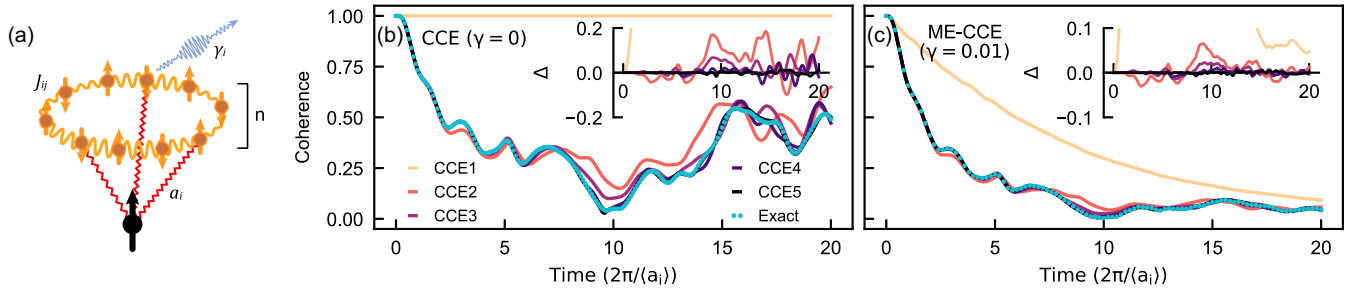


FIG. 1. Central spin coupled to a dissipative spin chain. Coherence refers to the coherence function  $\mathcal{L}(t)$  hereafter. (a) Schematic of a 12-spin chain ( $n = 12$ ) with uniformly distributed couplings  $J_{ij} \in [0, 0.2\pi]$ ,  $a_i \in [0, 4\pi]$  (see text). (b) Nondissipative spin chain. CCE1 to CCE5 denote the order of the expansion. Blue points correspond to the full numerical simulations. (c) Dissipative spin chain ( $\gamma = 0.01$ ). Insets of (b),(c) show the difference between the (ME-)CCE predictions and exact numerical simulations  $\Delta(t) = \mathcal{L}_{\text{CCE}}(t) - \mathcal{L}_{\text{exact}}(t)$  as a function of expansion order.

two ( $p = 2$ )  $\pi$  pulses applied to the central spin. We note that sequences with a higher number of pulses require higher expansion orders to obtain converged results.

The ME-CCE method allows us to study the decoherence of the central spin interacting with significantly larger chains, not tractable with exact methods. Figure 2(b) shows the decoherence of the central spin coupled to a chain with 200 spins ( $n = 200$ ) under different pulse sequences. Similar to the conventional CCE, the order required for convergence decreases as the size of the bath increases: the difference between truncating at the second or third order is negligible for all sequences studied here.

Finally, we find that the ME-CCE approach accurately captures the coherence dynamics even when collective dissipation is included in the simulation. For instance, we compute the dynamics of a chain with incoherent spin

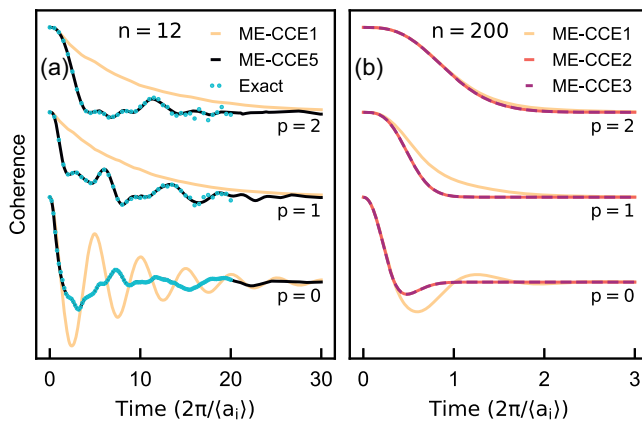


FIG. 2. Spin decoherence due to a spin chain under dynamical decoupling. (a) Decoherence of a spin coupled to a 12-spin chain as a function of number of the  $\pi$  pulses ( $p$ ) applied to the central spin. (b) Decoherence of a central spin coupled to a large spin chain. The coupling parameters are chosen in the same fashion as in Fig. 1(c).

exchange between nearest neighbors,  $\hat{L}_{i,\pm} = \hat{I}_{\mp}^i \otimes \hat{I}_{\pm}^{i+1}$  and we find that the ME-CCE results match the predictions of exact numerical simulations (see [28]).

Next, we investigate the decoherence of the central spin interacting with a two-dimensional dipolar-coupled square spin lattice [Fig. 3(a)]. In sensing applications, the electron spins commonly constitute the dominating spin bath at the surface of the host material [37]. Thus, we seek to understand whether the proposed approach is suitable to simulate the regime where the strength of the coupling between the central spin and the bath is comparable with that of intrabath interactions.

Such systems with no dissipative dynamics are challenging to simulate with the conventional CCE, requiring complex averaging procedures to reconstruct the coherence curve [38]. In contrast, we find that the presence of dissipative processes suppresses higher-order correlations, significantly *improving* the convergence of the ME-CCE method compared to CCE one [Figs. 3(b) and 3(c)]. Hence, the ME-CCE approach can be used to study spin baths with a wide range of intrabath coupling strengths.

Figure 3(d) shows the Hahn-echo signal of the central spin as a function of the bath-spin decay rate  $\gamma$ . To characterize the decoherence process, we use the coherence time  $T_2$ , defined as the time at which the coherence function decays to  $1/e$  of the initial value. We find that the coherence time varies nonmonotonically with  $\gamma$ : at low rates, it decreases with increasing  $\gamma$ , reaches a minimum near the coupling rate ( $\gamma \sim a_i$ ), and increases again at larger  $\gamma$ . The  $T_2$  enhancement in the large decay rate regime arises from the motional narrowing of the bath [39] and persists in systems with coupling extending beyond nearest neighbors [28]. These results for  $T_2$  provide a microscopic model explaining the coherence improvement observed experimentally in the case of a stochastic drive of the spin bath [40]. In this regime, the single spin contributions  $\mathcal{L}_i$  completely dominate the decoherence of the central spin. We can integrate Eq. (2) for a single bath spin, assuming the bath is in the infinite temperature limit, and we write  $\mathcal{L}_i$

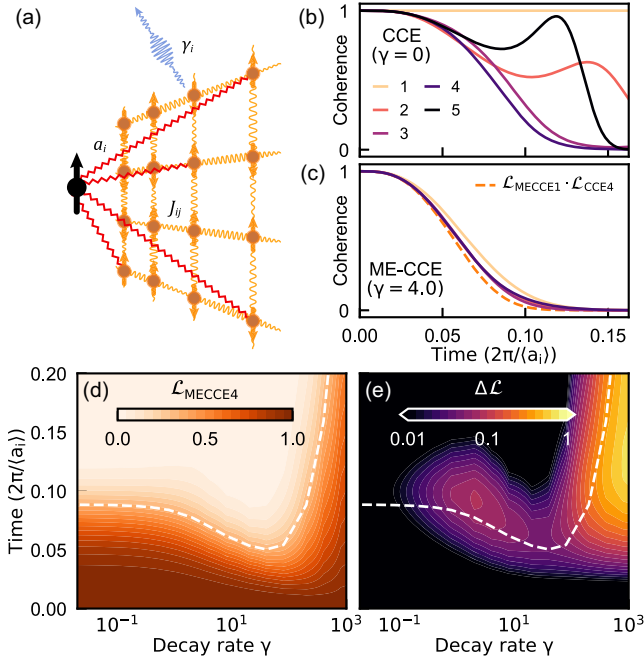


FIG. 3. Decoherence of a central spin coupled to a dissipative 2D lattice of spins. (a) Schematic representation of the system under study where  $J_{ij}$ ,  $a_i$ , and  $\gamma_i$  are defined as in Fig. 1. (b),(c) Hahn-echo signal in the system with (c) and without (b) dissipation. Different colors correspond to different approximation orders. (d) Hahn-echo coherence as a function of the bath spins decay rate. (e) Difference between full and factorized coherence function (see text) in the Hahn-echo experiment as a function of the bath-spin decay rate  $\gamma$ . For all plots, the spin bath has 400 spins ( $n = 400$ ) and starts from a random product state. Couplings are chosen as  $J_{ij} = 8\pi$ ,  $a_i \in [0, 4\pi]$ .

explicitly during the free evolution of the central spin as (see, e.g., [29]),

$$\mathcal{L}_i = e^{-\gamma_i t} \left( \cosh \left[ \frac{1}{2} \tilde{\omega}_i t \right] + \frac{2\gamma_i}{\tilde{\omega}_i} \sinh \left[ \frac{1}{2} \tilde{\omega}_i t \right] \right), \quad (6)$$

where  $\tilde{\omega}_i = \sqrt{4\gamma_i^2 - a_i^2}$ . In the small  $\gamma_i$  limit, the central spin coherence decays exponentially with a decay rate equal to  $\gamma_i$ , and in the large  $\gamma_i$  limit, the coherence decay rate is proportional to  $a_i^2/\gamma_i$ . At dissipation rates larger than the half coupling  $\gamma_i > (a_i/2)$ , the rhs of Eq. (6) is strictly real, and the dephasing rate of the central spin *decreases* with increased  $\gamma_i$ .

To investigate the interplay between spin relaxation and coherent spin exchange over a wide range of parameters, we compare the results of the full ME-CCE simulation at fourth order  $\mathcal{L}_{\text{MECCE4}}$  to the result obtained assuming two independent contributions. We compute the latter as a product of the contribution of the incoherent spin jumps from noninteracting spins, obtained with ME-CCE1, and the coherent spin exchange, computed with the conventional CCE at fourth order [ $\mathcal{L}_{\text{MECCE1}} \mathcal{L}_{\text{CCE4}}$  in Fig. 3(c)].

The difference  $\Delta\mathcal{L} = \mathcal{L}_{\text{MECCE4}} - \mathcal{L}_{\text{MECCE1}} \mathcal{L}_{\text{CCE4}}$  allows us to quantify the interplay between the two processes.

Figure 3(e) shows the difference in coherence curves  $\Delta\mathcal{L}$  as a function of the decay rate  $\gamma$ . We find that  $\Delta\mathcal{L}$  is strictly positive, i.e., the factorized coherence is smaller than or equal to the complete coherence function, indicating that an approximate treatment always predicts a faster coherence decay. The presence of dissipative dynamics thus effectively suppresses the coherent interactions in the bath and mitigates the effect of coherent processes on the central spin decoherence dynamics.

We note that only when the strength of the central-spin-bath interactions is comparable to both the strength of exchange interactions and that of the bath dissipation do we observe a strong deviation of  $\Delta\mathcal{L}$  from zero. In the regime where the couplings  $a_i$  are significantly larger than the exchange terms in the bath  $J_{ij}$ , the effects of the coherent interactions and incoherent spin flips on the central spin decoherence are almost entirely separable [28].

Finally, we apply our method to systems with practical relevance to sensing applications. We study the decoherence of the negatively charged nitrogen-vacancy (NV) center in diamond near the (100) surface [Fig. 4(a)]. The NV center is arguably the most studied and well-understood spin sensor [17,41], and the (100) surface is the most common facet used for sensing applications [15,42–44]. We assume that the surface contains  $0.001 \text{ nm}^{-2}$  dipolarly coupled electronic spins and that each surface spin has an intrinsic relaxation to a fully depolarized state with a lifetime of  $T_1 = 100 \mu\text{s}$ . This set of parameters is chosen to match the conditions reported in Ref. [15] and is consistent with other experimental measurements [45–48].

Under these conditions, the incoherent dynamics almost completely dominates the surface-induced decoherence of the NV center in the Hahn-echo experiment [Fig. 4(b)] [28]. We also find a different qualitative behavior of the coherence time, obtained with and without dissipative dynamics, as a function of the distance from the surface [Fig. 4(d)]. This result highlights the need to include dissipative dynamics of bath spins for all future first-principles studies of surface-induced decoherence.

*Discussion.*—In conclusion, we introduced a cluster-correlation expansion approach to solve the Lindblad master equation and compute the coherence of the central spin in a dissipative spin bath. Our approach reproduces the results of full numerical simulations for several 1D and 2D models and shows a remarkably robust convergence in a wide range of coupling parameters.

Our calculations revealed a rich interplay between Hamiltonian and dissipative dynamics in the bath and a nontrivial dependence of the central spin decoherence on the relaxation rate in the lattice, providing a microscopic model to explain the coherence improvements observed experimentally under stochastic driving of surface spins [40].

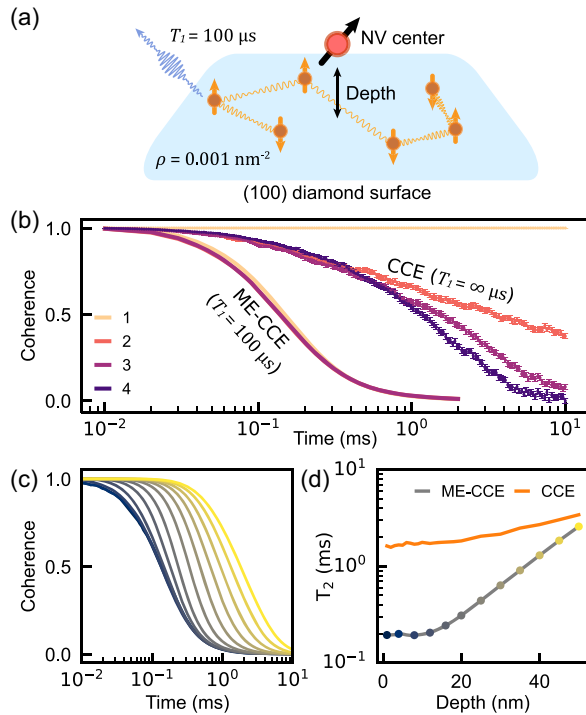


FIG. 4. Decoherence of a near-surface NV center in diamond. (a) Schematic representation of the system ( $\rho$  is the surface spin density,  $T_1$  is the relaxation time of the surface spins). (b) NV center Hahn-echo signal computed at various orders of the expansion at a distance of 10 nm from the surface. Solid lines (points) show results with (without) the dissipation of bath spins. (c) Coherence of the NV center as a function of the distance from the surface (0 to 50 nm, dark to light lines). (d) Coherence time  $T_2$ , obtained with the ME-CCE and CCE methods as a function of the distance from the surface.

We also investigated a shallow NV center near the (100) diamond surface and found that the surface spin's incoherent relaxation completely dominates the NV center's spin-echo decoherence in the experimentally observed range of parameters. This finding highlights the importance of including dissipative dynamical processes in first-principles simulations and motivates further in-depth studies.

We emphasize that the methodology presented here is general and applicable to any many-body open system coupled to a single probe, even with a non-Markovian environment [28]. Areas of interest include probing the spin squeezing with a single two-level system [49] in a dissipative environment, the interplay between phonon-limited relaxation and coherent spin exchange in bulk materials at high temperature, understanding the impact of incoherent spin hopping at surfaces, as well as quantifying the effect of the ensembles of two-level systems plaguing current superconducting devices [50], and the dynamics of multiple qubits in a hybrid cavity and circuit QED systems [51]. Finally, the CCE method has been shown to reliably reproduce many-body autocorrelation

functions [52,53], which now can be simulated even in a dissipative environment.

*Codes used.*—Full numerical simulations were carried out with QuTiP [54]. The ME-CCE approach is available as a part of the PyCCE package [30]. Specific scripts used are available on request from the authors.

We thank Jonathan Marcks for useful discussions. M. O., J. N., and G. G. acknowledge the support of NSF QuBQE Quantum Leap Challenge Institute (Grant No. NSF OMA-2121044). We also acknowledge partial support by the University of Chicago Materials Research Science and Engineering Center, which is funded by the National Science Foundation under Grant No. DMR-2011854. Code development in this work was supported by MICCoM, as part of the Computational Materials Sciences Program funded by the U.S. Department of Energy, Office of Science, Basic Energy Sciences, Materials Sciences, and Engineering Division through Argonne National Laboratory.

\*Corresponding author: gagalli@uchicago.edu

- [1] S. Diehl, A. Micheli, A. Kantian, B. Kraus, H. Büchler, and P. Zoller, Quantum states and phases in driven open quantum systems with cold atoms, *Nat. Phys.* **4**, 878 (2008).
- [2] F. Verstraete, M. M. Wolf, and J. Ignacio Cirac, Quantum computation and quantum-state engineering driven by dissipation, *Nat. Phys.* **5**, 633 (2009).
- [3] D. Witthaut, F. Trimborn, and S. Wimberger, Dissipation induced coherence of a two-mode Bose-Einstein condensate, *Phys. Rev. Lett.* **101**, 200402 (2008).
- [4] J. Eisert, M. Friesdorf, and C. Gogolin, Quantum many-body systems out of equilibrium, *Nat. Phys.* **11**, 124 (2015).
- [5] C. Noel, P. Niroula, D. Zhu, A. Risinger, L. Egan, D. Biswas, M. Cetina, A. V. Gorshkov, M. J. Gullans, D. A. Huse, and C. Monroe, Measurement-induced quantum phases realized in a trapped-ion quantum computer, *Nat. Phys.* **18**, 760 (2022).
- [6] C. Zu, F. Machado, B. Ye, S. Choi, B. Kobrin, T. Mittiga, S. Hsieh, P. Bhattacharyya, M. Markham, D. Twitchen, A. Jarmola, D. Budker, C. R. Laumann, J. E. Moore, and N. Y. Yao, Emergent hydrodynamics in a strongly interacting dipolar spin ensemble, *Nature (London)* **597**, 45 (2021).
- [7] M. Fitzpatrick, N. M. Sundaresan, A. C. Y. Li, J. Koch, and A. A. Houck, Observation of a dissipative phase transition in a one-dimensional circuit QED lattice, *Phys. Rev. X* **7**, 011016 (2017).
- [8] L.-N. Wu, J. Nettersheim, J. Feß, A. Schnell, S. Burgardt, S. Hiebel, D. Adam, A. Eckardt, and A. Widera, Indication of critical scaling in time during the relaxation of an open quantum system, *Nat. Commun.* **15**, 1714 (2024).
- [9] S. Diehl, E. Rico, M. A. Baranov, and P. Zoller, Topology by dissipation in atomic quantum wires, *Nat. Phys.* **7**, 971 (2011).
- [10] R. Ma, B. Saxberg, C. Owens, N. Leung, Y. Lu, J. Simon, and D. I. Schuster, A dissipatively stabilized Mott insulator of photons, *Nature (London)* **566**, 51 (2019).

- [11] Z.-P. Cian, G. Zhu, S.-K. Chu, A. Seif, W. DeGottardi, L. Jiang, and M. Hafezi, Photon pair condensation by engineered dissipation, *Phys. Rev. Lett.* **123**, 063602 (2019).
- [12] G. Akemann, M. Kieburg, A. Mielke, and T. c. v. Prosen, Universal signature from integrability to chaos in dissipative open quantum systems, *Phys. Rev. Lett.* **123**, 254101 (2019).
- [13] P. M. Harrington, E. J. Mueller, and K. W. Murch, Engineered dissipation for quantum information science, *Nat. Rev. Phys.* **4**, 660 (2022).
- [14] E. J. Davis, B. Ye, F. Machado, S. A. Meynell, W. Wu, T. Mittiga, W. Schenken, M. Joos, B. Kobrin, Y. Lyu, Z. Wang, D. Bluvstein, S. Choi, C. Zu, A. C. B. Jayich, and N. Y. Yao, Probing many-body dynamics in a two-dimensional dipolar spin ensemble, *Nat. Phys.* **19**, 836 (2023).
- [15] B. L. Dwyer, L. V. Rodgers, E. K. Urbach, D. Bluvstein, S. Sangtawesin, H. Zhou, Y. Nassab, M. Fitzpatrick, Z. Yuan, K. De Greve, E. L. Peterson, H. Knowles, T. Sumarac, J.-P. Chou, A. Gali, V. Dobrovitski, M. D. Lukin, and N. P. de Leon, Probing spin dynamics on diamond surfaces using a single quantum sensor, *PRX Quantum* **3**, 040328 (2022).
- [16] C. L. Degen, F. Reinhard, and P. Cappellaro, Quantum sensing, *Rev. Mod. Phys.* **89**, 035002 (2017).
- [17] J. F. Barry, J. M. Schloss, E. Bauch, M. J. Turner, C. A. Hart, L. M. Pham, and R. L. Walsworth, Sensitivity optimization for NV-diamond magnetometry, *Rev. Mod. Phys.* **92**, 015004 (2020).
- [18] D. M. Jackson, D. A. Gangloff, J. H. Bodey, L. Zaporski, C. Bachorz, E. Clarke, M. Hugues, C. Le Gall, and M. Atatüre, Quantum sensing of a coherent single spin excitation in a nuclear ensemble, *Nat. Phys.* **17**, 585 (2021).
- [19] D. A. Gangloff, L. Zaporski, J. H. Bodey, C. Bachorz, D. M. Jackson, G. Éthier Majcher, C. Lang, E. Clarke, M. Hugues, C. Le Gall, and M. Atatüre, Witnessing quantum correlations in a nuclear ensemble via an electron spin qubit, *Nat. Phys.* **17**, 1247 (2021).
- [20] W. Yang and R.-B. Liu, Quantum many-body theory of qubit decoherence in a finite-size spin bath, *Phys. Rev. B* **78**, 085315 (2008).
- [21] W. Yang, W.-L. Ma, and R.-B. Liu, Quantum many-body theory for electron spin decoherence in nanoscale nuclear spin baths, *Rep. Prog. Phys.* **80**, 016001 (2016).
- [22] H. Seo, A. L. Falk, P. V. Klimov, K. C. Miao, G. Galli, and D. D. Awschalom, Quantum decoherence dynamics of divacancy spins in silicon carbide, *Nat. Commun.* **7**, 12935 (2016).
- [23] S. Kanai, F. J. Heremans, H. Seo, G. Wolfowicz, C. P. Anderson, S. E. Sullivan, M. Onizhuk, G. Galli, D. D. Awschalom, and H. Ohno, Generalized scaling of spin qubit coherence in over 12, 000 host materials, *Proc. Natl. Acad. Sci. U.S.A.* **119**, e2121808119 (2022).
- [24] M. Onizhuk and G. Galli, Bath-limited dynamics of nuclear spins in solid-state spin platforms, *Phys. Rev. B* **108**, 075306 (2023).
- [25] A. Biella, J. Jin, O. Viyuela, C. Ciuti, R. Fazio, and D. Rossini, Linked cluster expansions for open quantum systems on a lattice, *Phys. Rev. B* **97**, 035103 (2018).
- [26] G. Lindblad, On the generators of quantum dynamical semigroups, *Commun. Math. Phys.* **48**, 119 (1976).
- [27] V. Gorini, A. Kossakowski, and E. C. G. Sudarshan, Completely positive dynamical semigroups of N-level systems, *J. Math. Phys. (N.Y.)* **17**, 821 (1976).
- [28] See Supplemental Material at <http://link.aps.org/supplemental/10.1103/PhysRevLett.132.250401> for discussion of convergence of ME-CCE, additional examples with nonuniform dissipation rates, incoherent spin exchange, diamond surface, and non-Markovian master equation, which includes Refs. [20,29–32].
- [29] P. Jurcevic and L. C. G. Govia, Effective qubit dephasing induced by spectator-qubit relaxation, *Quantum Sci. Technol.* **7**, 045033 (2022).
- [30] M. Onizhuk and G. Galli, pycce: A PYTHON package for cluster correlation expansion simulations of spin qubit dynamics, *Adv. Theory Simul.* **4**, 2100254 (2021).
- [31] S. John and T. Quang, Spontaneous emission near the edge of a photonic band gap, *Phys. Rev. A* **50**, 1764 (1994).
- [32] B. Donvil and P. Muratore-Ginanneschi, Quantum trajectory framework for general time-local master equations, *Nat. Commun.* **13**, 4140 (2022).
- [33] W. Yang and R.-B. Liu, Quantum many-body theory of qubit decoherence in a finite-size spin bath. II. Ensemble dynamics, *Phys. Rev. B* **79**, 115320 (2009).
- [34] S. Krämer and H. Ritsch, Generalized mean-field approach to simulate the dynamics of large open spin ensembles with long range interactions, *Eur. Phys. J. D* **69**, 282 (2015).
- [35] A. Vardi and J. R. Anglin, Bose-Einstein condensates beyond mean field theory: Quantum backreaction as decoherence, *Phys. Rev. Lett.* **86**, 568 (2001).
- [36] D. Witthaut, F. Trimborn, H. Hennig, G. Kordas, T. Geisel, and S. Wimberger, Beyond mean-field dynamics in open Bose-Hubbard chains, *Phys. Rev. A* **83**, 063608 (2011).
- [37] M. S. Grinolds, M. Warner, K. D. Greve, Y. Dovzhenko, L. Thiel, R. L. Walsworth, S. Hong, P. Maletinsky, and A. Yacoby, Subnanometre resolution in three-dimensional magnetic resonance imaging of individual dark spins, *Nat. Nanotechnol.* **9**, 279 (2014).
- [38] W. M. Witzel, M. S. Carroll, L. Cywiński, and S. Das Sarma, Quantum decoherence of the central spin in a sparse system of dipolar coupled spins, *Phys. Rev. B* **86**, 035452 (2012).
- [39] R. de Sousa, N. Shenvi, and K. B. Whaley, Qubit coherence control in a nuclear spin bath, *Phys. Rev. B* **72**, 045330 (2005).
- [40] M. Joos, D. Bluvstein, Y. Lyu, D. Weld, and A. B. Jayich, Protecting qubit coherence by spectrally engineered driving of the spin environment, *npj Quantum Inf.* **8**, 47 (2022).
- [41] R. Schirhagl, K. Chang, M. Loretz, and C. L. Degen, Nitrogen-vacancy centers in diamond: Nanoscale sensors for physics and biology, *Annu. Rev. Phys. Chem.* **65**, 83 (2014).
- [42] P. Maletinsky, S. Hong, M. S. Grinolds, B. Hausmann, M. D. Lukin, R. L. Walsworth, M. Loncar, and A. Yacoby, A robust scanning diamond sensor for nanoscale imaging with single nitrogen-vacancy centres, *Nat. Nanotechnol.* **7**, 320 (2012).
- [43] B. B. Zhou, P. C. Jerger, K.-H. Lee, M. Fukami, F. Mujid, J. Park, and D. D. Awschalom, Spatiotemporal mapping of a

- photocurrent vortex in monolayer MoS<sub>2</sub> using diamond quantum sensors, *Phys. Rev. X* **10**, 011003 (2020).
- [44] J.-P. Chou, P. Udvarhelyi, N. P. de Leon, and A. Gali, *Ab initio* study of (100) diamond surface spins, *Phys. Rev. Appl.* **20**, 014040 (2023).
- [45] A. O. Sushkov, I. Lovchinsky, N. Chisholm, R. L. Walsworth, H. Park, and M. D. Lukin, Magnetic resonance detection of individual proton spins using quantum reporters, *Phys. Rev. Lett.* **113**, 197601 (2014).
- [46] M. de Wit, G. Welker, J. M. de Voogd, and T. H. Oosterkamp, Density and  $T_1$  of surface and bulk spins in diamond in high magnetic field gradients, *Phys. Rev. Appl.* **10**, 064045 (2018).
- [47] Z. Zhang, M. Joos, D. Bluvstein, Y. Lyu, and A. C. Bleszynski Jayich, Reporter-spin-assisted  $T_1$  relaxometry, *Phys. Rev. Appl.* **19**, L031004 (2023).
- [48] K. Rezai, S. Choi, M. D. Lukin, and A. O. Sushkov, Probing dynamics of a two-dimensional dipolar spin ensemble using single qubit sensor, [arXiv:2207.10688](https://arxiv.org/abs/2207.10688).
- [49] M. Block, B. Ye, B. Roberts, S. Chern, W. Wu, Z. Wang, L. Pollet, E. J. Davis, B. I. Halperin, and N. Y. Yao, A universal theory of spin squeezing, [arXiv:2301.09636](https://arxiv.org/abs/2301.09636).
- [50] M. Carroll, S. Rosenblatt, P. Jurcevic, I. Lauer, and A. Kandala, Dynamics of superconducting qubit relaxation times, *npj Quantum Inf.* **8**, 132 (2022).
- [51] A. A. Clerk, K. W. Lehnert, P. Bertet, J. R. Petta, and Y. Nakamura, Hybrid quantum systems with circuit quantum electrodynamics, *Nat. Phys.* **16**, 257 (2020).
- [52] W. M. Witzel, K. Young, and S. Das Sarma, Converting a real quantum spin bath to an effective classical noise acting on a central spin, *Phys. Rev. B* **90**, 115431 (2014).
- [53] W.-L. Ma, G. Wolfowicz, S.-S. Li, J. J. L. Morton, and R.-B. Liu, Classical nature of nuclear spin noise near clock transitions of bi donors in silicon, *Phys. Rev. B* **92**, 161403(R) (2015).
- [54] J. Johansson, P. Nation, and F. Nori, QuTiP2: A PYTHON framework for the dynamics of open quantum systems, *Comput. Phys. Commun.* **184**, 1234 (2013).